THE JOURNAL OF PHYSICAL CHEMISTRY Letters

Letter

pubs.acs.org/JPCL

Unifying the 2e⁻ and 4e⁻ Reduction of Oxygen on Metal Surfaces

Venkatasubramanian Viswanathan,[†] Heine Anton Hansen,[‡] Jan Rossmeisl,[§] and Jens K. Nørskov*[,‡,∥]

[†]Department of Mechanical Engineering and [‡]Department of Chemical Engineering, Stanford University, Stanford, California 94305-3030, United States

[§]Center for Atomic-scale Materials Design, Department of Physics, Technical University of Denmark, DK-2800, Lyngby, Denmark

[∥]SUNCAT, SLAC National Accelerator Laboratory, Menlo Park, California 94025-7015, United States

Supporting Information

ABSTRACT: Understanding trends in selectivity is of paramount importance for multi-electron electrochemical reactions. The goal of this work is to address the issue of 2e⁻ versus 4e⁻ reduction of oxygen on metal surfaces. Using a detailed thermodynamic analysis based on density functional theory calculations, we show that to a first approximation an activity descriptor, ΔG_{OH^*}, the free energy of adsorbed OH*, can be used to describe trends for the 2e⁻ and 4e⁻ reduction of oxygen. While the weak binding of OOH* on Au(111) makes it an unsuitable catalyst for the 4e⁻ reduction, this weak binding is optimal for the 2e⁻ reduction to H_2O_2. We find quite a remarkable agreement between the predictions of the model and experimental results spanning nearly 30 years.

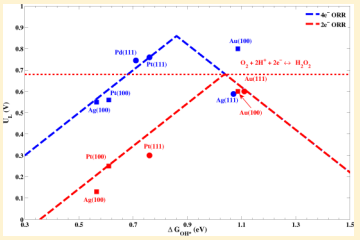

SECTION: Surfaces, Interfaces, Porous Materials, and Catalysis

Oxygen electrochemistry has gained paramount importance owing to its important role in fuel cells.[1] The electrocatalytic oxygen reduction reaction (ORR) on well-defined metal surfaces has been the subject of many experimental studies, and trends in electrocatalytic activity of the different facets are now well-established.[2−5] However, understanding the issue of selectivity of metal surfaces for the 2e⁻ reduction to H_2O_2 versus the 4e⁻ reduction to H_2O is less developed. A long-standing unsolved puzzle has been to understand the origin of structural effects for the 2e⁻ versus 4e⁻ reduction of oxygen. These structural effects were originally shown in the seminal work of Markovic et al.[3,4,6] and Behm et al.[7] Understanding the selectivity between H_2O_2 and H_2O would have a two-fold benefit: (1) It would help to enhance the performance of fuel cells where H_2O_2 is an undesirable product, significantly affecting the durability of fuel cells.[8] (2) It would also help in enhancing the efficiency of production of H_2O_2, a high-value chemical in the cleaning industry.[9] Additionally, understanding these trends could aid in better design for lithium-air batteries, where the selective 2e⁻ reduction of oxygen to Li_2O_2 is desired for rechargeable chemistry.[10]

Through the development of a semi-quantitative theoretical treatment of the free-energy diagrams of electrochemical reactions, it has become possible to construct volcano plots of activity as a function of adsorption energy. These volcano plots form a quantitative version of the Sabatier principle and have been used with success in the in-silico design of electrocatalysts, particularly for hydrogen evolution and 4e⁻ oxygen reduction.[11−13] However, for important multi-electron reactions such as CO_2 reduction and CH_3OH oxidation, active catalysts also need to be selective.[14] Therefore, understanding issues in selectivity represents the next frontier in the design of optimal electrocatalysts. Addressing the issue of selectivity computationally has been successful in a few simple cases in heterogeneous catalysis.[15−17] In this work, we demonstrate how to understand trends in selectivity for electrocatalytic oxygen reduction using a thermodynamic treatment.

An ideal electrocatalyst for the four-electron oxygen reduction should be able to facilitate reduction of O_2 just below the equilibrium potential of 1.23 V. In the case of oxygen reduction to H_2O, this requires as a minimum requirement that all of the four charge-transfer steps have reaction free energies of the same magnitude equal to the equilibrium potential of 1.23 eV.[18] Considering the associative mechanism shown below[18,19]

$$O_2(g) + 4H^+ + 4e^- + * \rightarrow OOH^* + 3H^+ + 3e^- \quad (1a)$$

$$OOH^* + 3H^+ + 3e^- \rightarrow O^* + H_2O(l) + 2H^+ + 2e^- \quad (1b)$$

$$O^* + H_2O(l) + 2H^+ + 2e^- \rightarrow OH^* + H_2O(l) + H^+ + e^- \quad (1c)$$

$$OH^* + H_2O(l) + H^+ + e^- \rightarrow * + 2H_2O(l) \quad (1d)$$

where * refers to a surface site. The electrocatalytic activity for 4e⁻ oxygen reduction is governed by the stability of intermediates OOH*, OH*, and O*. However, because of the existence of scaling relationships between these oxygen intermediates, the activity is governed by a single parameter and can be plotted as a function of OH* binding energy.[5,20] In the case of materials that bind oxygen intermediates too strongly, it has been shown that eq 1d, associated with the removal of

Received: September 20, 2012
Accepted: September 26, 2012
Published: September 26, 2012

adsorbed OH*, is the limiting step. Therefore, the free-energy difference of the limiting step is given by

$$\Delta G_{1d} = \Delta G_{H_2O(l)} - \Delta G_{OH^*} \quad (2)$$

In the case of the materials that bind oxygen intermediates too weakly, it has been shown that eq 1a, associated with the activation of O_2, is the limiting step. Therefore, the free energy difference of the limiting step is given by

$$\Delta G_{1a} = \Delta G_{OOH^*} - \Delta G_{O_2(g)} \quad (3)$$

An ideal electrocatalyst for the two electron reduction of oxygen should facilitate the reduction just below the equilibrium potential of 0.68 V. This implies that as a minimum requirement each of the two charge-transfer steps must have a reaction free energy of 0.68 eV. We consider a similar associative mechanism for H_2O_2 production

$$O_2(g) + 2H^+ + 2e^- + * \rightarrow OOH^* + H^+ + e^- \quad (4a)$$

$$OOH^* + H^+ + e^- \rightarrow H_2O_2(l) + * \quad (4b)$$

In this case, the activity of materials that bind oxygen intermediates too strongly, eq 4b, associated with the removal of OOH*, is the limiting step. The free energy of the limiting step is given by

$$\Delta G_{4b} = \Delta G_{H_2O_2(l)} - \Delta G_{OOH^*} \quad (5)$$

The activity of materials on the weak binding leg of the volcano is limited by eq 4a, associated with the activation of O_2, and the free-energy difference of the limiting step is given by

$$\Delta G_{4a} = \Delta G_{OOH^*} - \Delta G_{O_2(g)} \quad (6)$$

While the weak binding leg of the two electron and four electron reduction volcano is limited by the activation of O_2, the difference in the limiting step for the strong binding leg of the volcano between H_2O_2 and H_2O is associated with the removal of OOH* and OH*, respectively. The $2e^-$ reduction is governed by only one intermediate, OOH*, and thus, it is possible to find an electrocatalyst that binds OOH* optimally. Free-energy diagram for the $2e^-$ reduction of oxygen at a potential $U = 0.6$ V versus the reversible hydrogen electrode is shown in Figure 1. The calculated free energy of OOH* is based on density functional theory calculations, which accounts for stabilization from the water, electric field effects, zero point energy, and entropic corrections, and a detailed discussion is presented in the Supporting Information.[13] As can be seen from Figure 1, Au(111) is on the weak binding side with the limiting step being the activation of O_2. Pt(111) suffers from too strong a binding of OOH* and is limited by the reduction of OOH*. This is similar to previous findings by Mavrikakis et al.,[21] and this leads to a Sabatier volcano relationship as a function of the OOH* binding energy. It is to be noted that the surface coverage of H_{upd} at these potentials could play a role in modifying the activity for materials that bind OOH* strongly, such as Pt(111), as discussed extensively in the literature.[3] However, for the materials of interest for H_2O_2 production such as Au(111), the region of H_{upd} does not overlap with H_2O_2 production, and this effect is expected to be minimal. A more detailed discussion of this is given in the Supporting Information.

Recently, it has been shown that the free-energy difference between OH* and OOH* is constant within ±0.2 eV and appears to be universal, independent of the binding strength to the surface.[22] This observation was made by Koper,[23] where he noted that the binding strengths of OH* and OOH* are related to each other by a constant amount of ~3.2 eV for metal (111) facets and oxide surfaces regardless of the binding site. We have recently shown using detailed density functional theory calculations that this scaling relation also holds for metal (100) facets.[5] As a result, we can combine the thermodynamic analysis for the $2e^-$ and $4e^-$ reduction and describe the activity, to a first approximation, as a function of a single descriptor, ΔG_{OH^*}.

An activity plot based on the thermodynamic analysis is shown in Figure 2, and we have made a comparison of our model for the activity to several rotating ring disk electrode (RRDE) experiments on well-defined metal (111) and (100) surfaces. The activity volcano is plotted between the potential

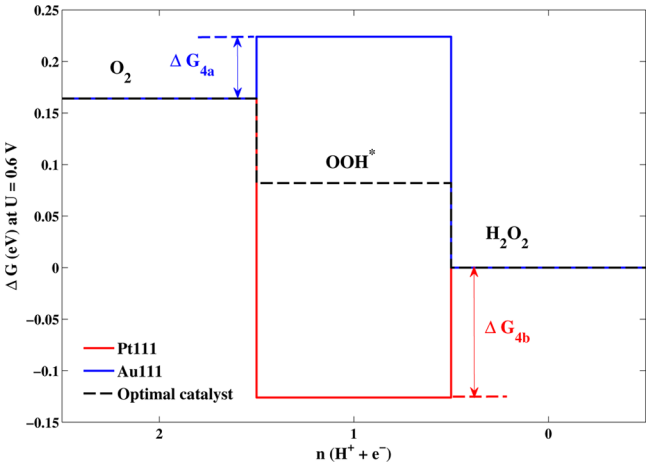

Figure 1. Free-energy diagram of $2e^-$ oxygen reduction reaction plotted at $U = 0.6$ V versus the reversible hydrogen electrode. The limiting step for Au(111) is the activation of O_2 to OOH*, whereas that for Pt(111) is the reduction of OOH* to H_2O_2.

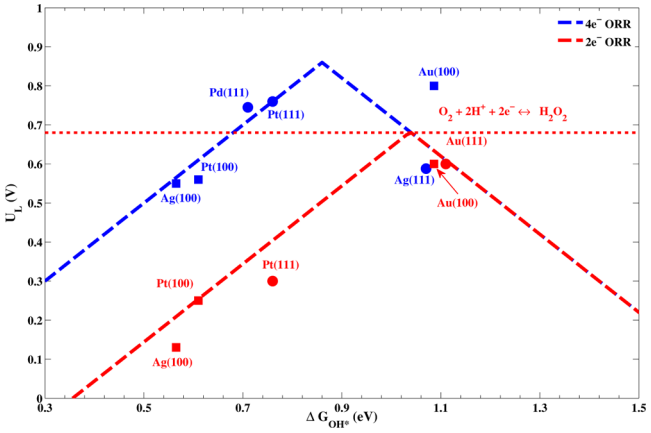

Figure 2. Activity volcanoes for the $2e^-$ and $4e^-$ reduction of oxygen are shown in red and blue respectively. The experimental data for the $2e^-$ and $4e^-$ reduction of oxygen are taken from Markovic et al.[24] for Pt(111) and Pt(100), Shao et al.[29] for Pd(111), Blizanac et al.[4] for Ag(111) and Ag(100), Blizanac et al.[30] for Au(100), and Schmidt et al.[3] for Au(111). The experimental value of the limiting potential, U_L, is determined by the half-wave potentials for the $4e^-$ reduction and by the onset of ring current for the $2e^-$ reduction. The equilibrium potential for H_2O_2 formation is shown as a dashed line. The activity of (111) and (100) surfaces has been plotted in circles and squares, respectively.

dx.doi.org/10.1021/jz301476w | J. Phys. Chem. Lett. 2012, 3, 2948−2951

limiting step, U_L, the highest potential where all of the steps are downhill in free energy, and the free energy of adsorbed OH*. In a RRDE experiment, the disk current and ring current can be used to determine the selectivity of reduction to H_2O and H_2O_2, respectively. The experimental measurements in acidic environment considered for comparison are all carried out in 0.1 M $HClO_4$, and the experimental measurement of Au(100) and Au(111) in alkaline environment is carried out in 0.1 M KOH. All experiments are carried out at a rotation speed of 1600 rpm except for Au(111), which was carried out at 2500 rpm. We note that changes in rotation speed cause only a small change in half-wave potential of ~20 mV.[24,25] The choice of $HClO_4$ as the electrolyte is made because it is a nonadsorbing electrolyte and does not compete with the oxygen intermediates for adsorption.[26] We have intentionally avoided H_2SO_4 and HCl because bisulphate and chloride ions are known to adsorb strongly on fcc metal surfaces.[27,28] It has been demonstrated in the work of Markovic and coworkers that adsorbed spectator species, such as Cl_{ads} and $HSO_{4,ads}$, significantly changes the activity of Pt(hkl) surfaces for $2e^-$ and $4e^-$ reduction.[27]

The half-wave potentials have been used to plot the experimental activity for the $4e^-$ reduction, and the onset of ring current has been used to plot the experimental activity for the $2e^-$ reduction. The direct comparison to the experimental half-wave potential can be made by including a prefactor to the calculated theoretical overpotential. We have chosen to match the experimental half-wave potential to the calculated theoretical overpotential on Pt(111). This is done to be consistent with previous oxygen reduction volcano plots.[12,13] The calculated theoretical overpotential for Pt(111) is 0.76 V, and the experimental half-wave potential is 0.82 V.[24] The limiting potentials are plotted relative to this choice of prefactor which results in a 60 mV shift for the $4e^-$ reduction from the experimental half-wave potential.

We find quite a remarkable agreement between the results of the model and experiments given the simplicity of the model. We find that a similar trend is maintained among Pt(111), Pt(100), and Ag(100) for the $2e^-$ and $4e^-$ reduction. The shift in the $2e^-$ and $4e^-$ reduction of oxygen on the strong binding leg is governed by the free-energy difference between OOH* and OH*. The constant trend for the strong binding materials is an indirect experimental evidence of the constant scaling between OOH* and OH*. On the weak binding leg, we find that Au(111) is an excellent catalyst with a very small overpotential. While the weak binding of OOH* on Au(111) makes it an unsuitable catalyst for $4e^-$ reduction, the binding of OOH* is nearly optimal for the $2e^-$ reduction. It is to be noted that Au(111) is quite close to the top of the volcano, and within the accuracy of our calculations, it is hard to conclusively assign Au(111) to the left or right side of the volcano. This is in good agreement with the experiments of Schmidt et al., where it shown that significant ring and ORR current is observed at ~0.6 V.[3] Within our model, we attribute the enhanced activity of Au(100) for the $4e^-$ reduction to a stronger binding of oxygen intermediates relative to Au(111). However, at a slightly lower potential of ~0.6 V, Au(100) produces substantial ring current consistent with our model. Within the accuracy of our calculations, we demonstrate that Au(100) is also near the top of the $2e^-$ reduction volcano. However, it is difficult to assign it conclusively to the left or right side of the volcano.

Finally, we note that the choice of ΔG_{OH^*} as the descriptor is intentional to aid an easier identification of active electrocatalysts experimentally. We have shown that the location of the first oxidative peak in a cyclic voltammogram in N_2 environment can be used to determine ΔG_{OH^*},[31] and the position of the first oxidative peak obtained from cyclic voltammograms has been used directly to correlate with the $4e^-$ oxygen reduction activity.[20]

The success of this simple thermodynamic treatment in rationalizing trends of selectivity lends great hope to the in-silico design of selective electrocatalysts. It is imperative to address trends in selectivity when designing electrocatalysts for key multielectron reactions such as CO_2 reduction. Therefore, we expect the principles that we have developed in the thermodynamic theory of multielectron reactions to be crucial in the design of selective, stable electrocatalysts.

■ ASSOCIATED CONTENT

Supporting Information

Detailed discussion of the procedure of calculating the thermodynamics of reaction intermediates, the issue of the surface structure of the (100) facets, and the role of H_{upd}. This material is available free of charge via the Internet http://pubs.acs.org/.

■ AUTHOR INFORMATION

Corresponding Author

*E-mail: norskov@stanford.edu.

Notes

The authors declare no competing financial interest.

■ ACKNOWLEDGMENTS

We acknowledge support from the Department of Energy, Basic Energy Sciences through the SUNCAT Center for Interface Science and Catalysis and V.V. for the UTRC fellowship. We would also like to thank a referee of a previous manuscript who brought this puzzle to our attention.

■ REFERENCES

(1) Markovic, N. M.; Ross, P. N. Surface Science Studies of Model Fuel Cell Electrocatalysts. *Surf. Sci. Rep.* **2002**, *45*, 117−229.

(2) Markovic, N. M.; Ross, P. N., Jr. In *Interfacial Electrochemistry: Theory, Experiments and Applications*; Wieckowski, A., Ed.; Marcel Dekker: New York, 1999; p 821.

(3) Schmidt, T.; Stamenkovic, V.; Arenz, M.; Marković, N. M.; Ross, P. N. Oxygen Electrocatalysis in Alkaline Electrolyte: Pt(hkl), Au(hkl) and the Effect of Pd-Modification. *Electrochim. Acta* **2002**, *47*, 3765−3776.

(4) Blizanac, B.; Ross, P. N.; Marković, N. M. Oxygen Reduction on Silver Low-index Single-Crystal Surfaces in Alkaline Solution: Rotating Ring Disk(Ag(hkl)) Studies. *J. Phys. Chem. B* **2006**, *110*, 4735−4741.

(5) Viswanathan, V.; Hansen, H. A.; Rossmeisl, J.; Nørskov, J. K. Universality in Oxygen Reduction Electrocatalysis on Metal Surfaces. *ACS Catal.* **2012**, *2*, 1654−1660.

(6) Marković, N. M.; Adzic, R. R.; Vesovic, V. B. Structural Effects in Electrocatalysis: Oxygen Reduction on the Gold Single Crystal Electrodes with (110) and (111) Orientations. *J. Electroanal. Chem.* **1984**, *165*, 121−133.

(7) Jusys, Z.; Behm, R. J. Simulated "Air Bleed" Oxidation of Adsorbed CO on Carbon Supported Pt. Part 2. Electrochemical Measurements of Hydrogen Peroxide Formation during O_2 Reduction in a Double-Disk Electrode Dual Thin-layer Flow Cell. *J. Phys. Chem. B* **2004**, *108*, 7893−7901.

(8) Behm, R. J.; Jusys, Z. The Potential of Model Studies for the Understanding of Catalyst Poisoning and Temperature Effects in

Polymer Electrolyte Fuel Cell Reactions. *J. Power Sources* **2006**, *154*, 327−342.
(9) Drogui, P.; Elmaleh, S.; Rumeau, M.; Bernard, C.; Rambaud, A. Hydrogen Peroxide Production by Water Electrolysis: Application to Disinfection. *J. Appl. Electrochem.* **2001**, *31*, 877−882.
(10) Bruce, P. G.; Freunberger, S. A.; Hardwick, L. J.; Tarascon, J.-M. Li-O-2 and Li-S Batteries with High Energy Storage. *Nat. Mater.* **2012**, *11*, 19−29.
(11) Greeley, J.; Jaramillo, T. F.; Bonde, J.; Chorkendorff, I. B.; Nørskov, J. K. Computational High-throughput Screening of Electrocatalytic Materials for Hydrogen Evolution. *Nat. Mater.* **2006**, *5*, 909−913.
(12) Stamenkovic, V.; Mun, B. S.; Mayrhofer, K. J. J.; Ross, P. N.; Markovic, N. M.; Rossmeisl, J.; Greeley, J.; Nørskov, J. K. Changing the Activity of Electrocatalysts for Oxygen Reduction by Tuning the Surface Electronic Structure. *Angew. Chem., Int. Ed.* **2006**, *45*, 2897−2901.
(13) Greeley, J.; Stephens, I.; Bondarenko, A.; Johansson, T.; Hansen, H. A.; Jaramillo, T.; Rossmeisl, J.; Chorkendorff, I.; Nørskov, J. Alloys of Platinum and Early Transition Metals as Oxygen Reduction Electrocatalysts. *Nat. Chem.* **2009**, *1*, 552−556.
(14) Peterson, A. A.; Abild-Pedersen, F.; Studt, F.; Rossmeisl, J.; Nørskov, J. K. How Copper Catalyzes the Electroreduction of Carbondioxide into Hydrocarbon Fuels. *Energ. Environ. Sci.* **2010**, *3*, 1311−1315.
(15) Linic, S.; Jankowiak, J.; Barteau, M. A. Selectivity Driven Design of Bimetallic Ethylene Epoxidation Catalysts from First Principles. *J. Catal.* **2004**, *224*, 489−493.
(16) Christopher, P.; Linic, S. Engineering Selectivity in Heterogeneous Catalysis: Ag Nanowires as Selective Ethylene Epoxidation Catalysts. *J. Am. Chem. Soc.* **2008**, *130*, 11264−11265.
(17) Studt, F.; Abild-Pedersen, F.; Bligaard, T.; Sorensen, R. Z.; Christensen, C. H.; Nørskov, J. K. Identification of Non-precious Metal Alloy Catalysts for Selective Hydrogenation of Acetylene. *Science* **2008**, *320*, 1320−1322.
(18) Nørskov, J. K.; Rossmeisl, J.; Logadottir, A.; Lindqvist, L.; Kitchin, J. R.; Bligaard, T.; Jonsson, H. Origin of the Overpotential for Oxygen Reduction at a Fuel-Cell Cathode. *J. Phys. Chem. B* **2004**, *108*, 17886−17892.
(19) Karlberg, G. S.; Rossmeisl, J.; Nørskov, J. K. Estimations of Electric Field Effects on the Oxygen Reduction Reaction Based on the Density Functional Theory. *Phys. Chem. Chem. Phys.* **2007**, *9*, 5158−5161.
(20) Stephens, I. E. L.; Bondarenko, A. S.; Perez-Alonso, F. J.; Calle-Vallejo, F.; Bech, L.; Johansson, T. P.; Jepsen, A. K.; Frydendal, R.; Knudsen, B. P.; Rossmeisl, J.; Chorkendorff, I. Tuning the Activity of Pt(111) for Oxygen Electroreduction by Subsurface Alloying. *J. Am. Chem. Soc.* **2011**, *133*, 5485−5491.
(21) Ford, D. C.; Nilekar, A. U.; Xu, Y.; Mavrikakis, M. Partial and Complete Reduction of O_2 by Hydrogen on Transition Metal Surfaces. *Surf. Sci.* **2010**, *604*, 1565−1575.
(22) Man, I.; Su, H.; Calle-Vallejo, F.; Hansen, H. A.; Martnez, J.; Inoglu, N.; Kitchin, J.; Jaramillo, T.; Nørskov, J.; Rossmeisl, J. Universality in Oxygen Evolution Electrocatalysis on Oxide Surfaces. *ChemCatChem* **2011**, *3*, 1159−1165.
(23) Koper, M. T. M. Thermodynamic Theory of Multi-Electron Transfer Reactions: Implications for Electrocatalysis. *J. Electroanal. Chem.* **2011**, *660*, 254−260.
(24) Marković, N. M.; Gasteiger, H. A.; Ross, P. N. Kinetics of Oxygen Reduction on Pt(hkl) Electrodes: Implications for the Crystallite Size Effect with Supported Pt Electrocatalysts. *J. Electrochem. Soc.* **1997**, *144*, 1591−1597.
(25) Wang, J. X.; Markovic, N. M.; Adzic, R. R. Kinetic Analysis of Oxygen Reduction on Pt(111) in Acid Solutions: Intrinsic Kinetic Parameters and Anion Adsorption Effects. *J. Phys. Chem. B* **2004**, *108*, 4127−4133.
(26) Bondarenko, A. S.; Stephens, I. E. L.; Hansen, H. A.; Pérez-Alonso, F. J.; Tripkovic, V.; Johansson, T. P.; Rossmeisl, J.; Nørskov, J. K.; Chorkendorff, I. The Pt(111)/Electrolyte Interface under Oxygen Reduction Reaction Conditions: An Electrochemical Impedance Spectroscopy Study. *Langmuir* **2011**, *27*, 2058−2066.
(27) Markovic, N. M.; Schmidt, T. J.; Stamenkovic, V.; Ross, P. N. Oxygen Reduction Reaction on Pt and Pt Bimetallic Surfaces: A Selective Review. *Fuel Cells* **2001**, *1*, 105−116.
(28) Halseid, R.; Heinen, M.; Jusys, Z.; Behm, R. J. The Effect of Ammonium Ions on Oxygen Reduction and Hydrogen Peroxide Formation on Polycrystalline Pt Electrodes. *J. Power Sources* **2008**, *176*, 435−443.
(29) Shao, M.; Huang, T.; Liu, P.; Zhang, J.; Sasaki, K.; Vukmirovic, M.; Adzic, R. R. Palladium Monolayer and Palladium Alloy Electrocatalysts for Oxygen Reduction. *Langmuir* **2006**, *22*, 10409−10415.
(30) Blizanac, B.; Lucas, C.; Gallagher, M.; Arenz, M.; Ross, P.; Markovic, N. Anion Adsorption, CO Oxidation, and Oxygen Reduction Reaction on a Au(100) Surface: The pH Effect. *J. Phys. Chem. B* **2004**, *108*, 625−634.
(31) Viswanathan, V.; Hansen, H. A.; Rossmeisl, J.; Jaramillo, T.; Pitsch, H.; Nørskov, J. K. Simulating Linear Sweep Voltammetry from First-Principles: Application to Electrochemical Oxidation of Water on Pt(111) and $Pt_3Ni(111)$. *J. Phys. Chem. C* **2012**, *116*, 4698−4704.